Journal of Thermal Analysis, Vol. 48 (1997) 951-969

INTRINSIC THERMAL STABILITY AND QUENCHING RECOVERY OF THIN-FILM SUPERCONDUCTORS WITH THERMAL BOUNDARY RESISTANCE

J.-P. Wu and H.-S. Chu

Department of Mechanical Engineering, National Chiao Tung University, Hsinchu, Taiwan 300, Republic of China

Abstract

The stability behaviour of a thin-film superconductor under a localized release of thermal disturbance is investigated. Two-dimensional conjugate film/substrate conduction equation with anisotropic thermal conductivity of the film, and Joule heat are employed to investigate effects of substrate and thermal properties on the intrinsic stability and quenching recovery. To consider the thermal boundary resistance between film and substrate, an interfacial-layer model (ILM) with very low diffusivity and an acoustic mismatch model (AMM) are employed. Results show that the thermal boundary resistance influences strongly the intrinsic stability. Thermal boundary resistance increases intrinsic stability if the thermal conductivity of the substrate or the disturbance energy is large. Higher Biot numbers and thermal conductivity ratios of film to substrate in longitudinal direction influence stability favorably. We demonstrate also that operation of a film/substrate system, such as YBCO/MgO, is either intrinsically stable or irrecoverably unstable.

Keywords: thermal boundary resistance, thermal stability, thin-film superconductor

Introduction

The stability in the presence of thermal disturbances is one of the most important problems in the application of thin-film superconductors. The thermal disturbances are most likely due to transient, localized, point-source heat releases and are produced by various mechanisms, such as sudden relaxation of dislocations, crystal defects, and other spontaneous processes in superconductors [1–2]. The energy can increase the temperature level of the superconductor to the transition point where superconductors stop superconducting state and become normal resistive materials, a phenomenon known as quenching. As the local temperature is raised, the critical current density is reduced, in turn, the current is distributed to the other undisturbed region. If the operating current can not be accepted by the undisturbed region, Joule heating will occur. To keep the superconductors superconducting, it is necessary to provide adequate heat transfer after the occurrence of thermal disturbances and Joule heating. Understanding the heat transfer behavior of superconductor film/substrate composite, which is therefore of great importance.

The thermal properties of substrates are important factors which affects significantly the thermal stability of superconductors. Generally, larger substrates with

0368–4466/97/ $ 5.00

John Wiley & Sons Limited
Chichester

better thermal conductivity will be considered good heat sinks, and increase in size also increase their heat capacities. Therefore, substrate effects are not negligible.

In addition to substrate effects, the thermal boundary resistance between the superconducting thin film and the substrate also greatly affects the thermal stability. The existence of thermal resistance diminishes the substrate effects and heat generated in the film is conducted to the substrate with difficulty. Wetzko *et al.* [3] dealt with the stability of Bi-2223/Ag, transport current distribution and current-sharing in considering thermal boundary resistance. They found that the influence of thermal boundary resistance on intrinsic stability was small, since metal/ceramic contact resistance is very small. But their results are not applicable to our research on the structure of superconducting thin films deposited on oxide substrates. Streiffer *et al.* [4] indicated that a significant thermal barrier can exist at the interface of an YBCO/MgO system. Swartz and Pohl [5] showed that the contact resistance increases greatly in the cases where definite surface roughness is present and if diffuse phonon scattering limits heat transfer at the interface. Marshall *et al.* [6] not only reported that a temperature-dependent thermal barrier significantly restricts heat transfer from the film into the substrate, but also quantified this thermal boundary resistance. They stated that the rate of flow through the YBCO/MgO interface is about 100 times less than the rate of flow in the YBCO film. Moreover, they showed the barrier to thermal flow at the MgO substrate interface has a thickness of the order of a unit-cell size of ~11 Å. At present, at least two different models are used to predict thermal boundary resistance. The first model assumes a radiation boundary conditions in which the thermal flow across the interface is proportional to the difference of the fourth power of the temperature on each side of the interface [7]. This approximation is based on the acoustic mismatch model (AMM). However, the AMM has been found to be in agreement with measurements only for temperatures below ~30 K [5]. When the temperature increases, the thermal boundary resistance does not continue to decrease with T^{-3}, but instead approaches a constant value at the higher temperature. Nahum *et al.* [8] recently measured the thermal boundary resistance between $YBa_2Cu_3O_{7-\delta}$ thin films and several substrates, and found it to be larger by a factor of ~80 at 100 K than the resistance derived from the AMM. Thus at temperatures above ~50 K, the AMM should not be employed, whereas in this paper the AMM is offered to be compared with the anther model as mentioned below. The second model, the interfacial layer model (ILM) assumes an interfacial layer of variable thickness exists inside the superconducting film, and that the diffusivity of it is significantly lower (~10–100 times) than that of bulk YBCO [6]. Chen *et al.* [9] were the first to employ the two models for theoretical analysis of an YBCO/substrate thermal system.

Most previous analyses of thermal stability concerned normal-zone behavior after normal cross-section formation, and were based on considering one-dimensional heat conduction along the electric current or in the longitudinal direction [10–15]. If an transient point-source releases heat, the cross-sectional area where the point-source is located will normalize first. Subsequently, this area will grow further into a normal zone in a longitudinal direction, if sufficient heat is not trans-

ferred away to the coolant or/and stabilizer. The normal zone is always most pronounced at the center of the length of a longitudinal line-source disturbance of any length. Therefore, the stability performance of the superconductors as regards normal zone behaviour at such central cross-sectional area across the transverse direction is important. Flik and Tien [2] defined an intrinsic stability criterion for a normal cross-section of bare film. Intrinsic thermal stability describes the condition in which a superconductor can carry the operating current without Joule heating for an unlimited time after a localized release of thermal energy. Chen and Chu [16] presented a three-dimensional analysis that considered an instantaneous release of energy by a finite-length line source. They also showed that the anisotropy of oriented films has a great impact on thermal stability. On the basis of previous works, Unal and Chyu [17] investigated the phenomenon of superconductivity recovery after failure of stability and defined the recovery criterion. They provided an explanation of two distinct types of behavior exhibited during recovery of superconductivity after quenching. Seol and Chyu [18] investigated current sharing with the stabilizer and the possible recovery of superconductivity for a one-dimensional composite-tape superconductor, and developed stability criterion based on heat conduction analyses for the current-sharing steady state and quenching steady state. However, previous studies have not simultaneously considered the substrate effects and thermal boundary resistances in analyzing thermal stability.

The present paper investigates the intrinsic thermal stability and quench-recovery characteristics of film/substrate superconductor systems. Two-dimensional heat conduction equations with an instantaneous release of energy in the form of infinite length of line source at the center of the cross-section of the superconductor is considered. The quench-recovery behavior, substrate effects, and heat transfer coefficient of coolant are discussed. Two important critical current density ratios are also calculated. The first critical current density, $(J_r)_{c1}$, above which the intrinsic thermal stability fails and Joule heat is generated, can be determined according to the intrinsic stability theory [2]. The second critical current density, $(J_r)_{c2}$, beyond which recovery of thermal stability is impossible, can be found using the recovery criterion and a steady-state-temperature solution under Joule heating [17]. Both the AMM and the ILM are employed in considering the effects of thermal boundary resistance on thermal stability. Results from this work show that the ILM exerts a stronger influence on thermal stability than the AMM at 77 K. The values of $(J_r)_{c1}$, when the effects of thermal boundary resistance are ignored, are significantly underestimated for higher E_d and K_{fs}, and Bi. By contrast, the variation in $(J_r)_{c2}$ is slight for different Bi and K_{fs}.

Analysis

The physical system under consideration is shown in Fig. 1. A thin-film superconductor of thickness d_f is deposited on a substrate of thickness d_s, their widths are $2a$. An infinite length of line heat source is located at point (x_o, y_o) of the cross-section normal to current direction. At time $t=0$, a finite amount of thermal energy,

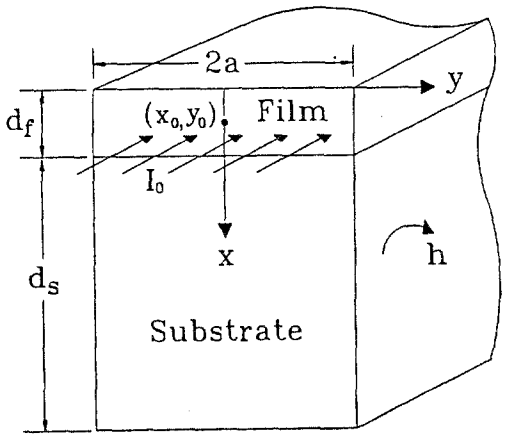

Fig. 1 The physical model of thin-film superconductor deposited on substrate

e_o, is released. The heat transfer coefficient h between the superconductor and the surrounding coolant is assumed to be constant and uniform. The coolant is maintained at the operating temperature T_o. The operating electrical current, I_o, flows through the conductor normal to the xy plane. No magnetic field is assumed to be presented, as in typical electronics applications.

Intrinsic thermal stability

The thin-film superconductor-substrate system can be described by the following transient heat diffusion equations:

$$\text{for the thin film: } \rho_f c_f \frac{\partial T_f}{\partial_t} = \nabla(K\nabla T)_f \tag{1}$$

$$\text{for the substrate: } \rho_s c_s \frac{\partial T_s}{\partial_t} = \nabla(K\nabla T)_s \tag{2}$$

where K is the conductivity tensor. Most ceramic high-temperature superconductors are highly anisotropic. In this study, we consider the anisotropic of thermal conductivity of film, and assume the thermal conductivity remain constant above 77 K [19].

Using two-dimensional Cartesian coordinates, the following nondimensional parameters are introduced to obtain a more compact form of the Fourier equation.

$$\theta_f = \frac{T_f - T_o}{T_c - T_o}, \quad \theta_s = \frac{T_s - T_o}{T_c - T_o}, \quad \tau = \frac{k_{fx} t}{d_f^2 \rho_f c_f} \tag{3a}$$

$$X = \frac{x}{d_f}, \qquad Y = \frac{y}{d_f\sqrt{K_r}}, \qquad \alpha_r = \frac{\alpha_{fx}}{\alpha_s} = \frac{k_{fx}/\rho_f c_f}{k_s/\rho_s c_s} \tag{3b}$$

$$A = \frac{A_r}{\sqrt{K_r}}, \qquad A_r = \frac{a}{d_f}, \qquad D = \frac{d_s}{d_f} \tag{3c}$$

$$K_r = \frac{k_{fy}}{k_{fx}}, \qquad K_{fs} = \frac{k_{fx}}{k_s}, \qquad Q_b = \frac{q_b d_f}{k_{fx}(T_c - T_o)} \tag{3d}$$

Substituting Eqs (3a–3d) into the associated equations renders an isotropic form of the Fourier equation for thin film. The energy equations are as follows:

$$\frac{\partial\theta_f}{\partial\tau} = \frac{\partial^2\theta_f}{\partial X^2} + \frac{\partial^2\theta_f}{\partial Y^2} \qquad 0 < X < 1, \quad -A < Y < A \tag{4}$$

$$\frac{\partial\theta_s}{\partial\tau} = \frac{1}{\alpha_r}\frac{\partial^2\theta_s}{\partial X^2} + \frac{1}{K_r\alpha_r}\frac{\partial^2\theta_s}{\partial Y^2} \qquad 1 < X < 1 + D, \quad -A < Y < A \tag{5}$$

The associated boundary conditions become:

$$\frac{\partial\theta_f}{\partial X} = Bi\theta_f \qquad \text{at } X = 0 \tag{6a}$$

$$-\frac{\partial\theta_f}{\partial X} = -\frac{1}{K_{fs}}\frac{\partial\theta_s}{\partial X}, \quad -\frac{\partial\theta_f}{\partial X} = Q_b \qquad \text{at } X = 1 \tag{6b}$$

$$-\frac{\partial\theta_s}{\partial X} = BiK_{fs}\theta_s \qquad \text{at } X = 1 + D \tag{6c}$$

$$\pm\frac{\partial\theta_f}{\partial Y} = \frac{Bi}{\sqrt{K_r}}\theta_f \qquad \text{at } Y = \pm A \tag{6d}$$

$$\pm\frac{\partial\theta_s}{\partial Y} = BiK_{fs}\sqrt{K_r}\theta_s \qquad \text{at } Y = \pm A \tag{6e}$$

where $Bi = hd_f/k_{fx}$ and the initial condition is in the form

$$\int_{-A}^{A}\int_{0}^{1}\theta_f dX dY = 2E_d A \qquad \text{for } \tau = 0 \tag{7}$$

$$\theta_f = 2\delta(X - X_o)\delta(Y - Y_o)E_d A \qquad \text{for } 0 \le X_o \le 1, \quad -A \le Y_o \le A \tag{8}$$

where

$$E_d = \frac{e_d}{\rho_f c_f (T_c - T_o) 2ad_f} \tag{9}$$

If the thermal disturbance is located at the center of the cross-section, the principle of symmetry allows us to consider only half the $X>0, Y>0$ region, and to assume adiabatic boundary conditions at the planes of symmetry. For numerical calculation we prescribe that energy is initially deposited in an area of $4\Delta x \times \Delta y$, for which the dimensionless form is

$$\theta_f(X,Y,0) = \begin{cases} \theta_d, & 0.5 - \Delta X \le X \le 0.5 + \Delta X, \quad 0 \le Y \le \Delta Y \\ 0, & \text{others} \end{cases} \tag{10}$$

where θ_d is a normalized temperature which represents the amount of thermal disturbance. It is defined as

$$\theta_d = \frac{E_d A}{2\Delta X \Delta Y} \tag{11}$$

Two models are offered to estimate the thermal boundary resistance between the film and the substrate, as follows:

Radiation-boundary-condition model

This approximation is based on the AMM [7], which is in agreement with measurements below 30 K. If this model is employed, the following equations are introduced into the boundary condition in Eq. (6b).

$$q_b = \kappa(T_f^4 - T_s^4) \tag{6b'}$$

$$\kappa = \frac{2\pi \bar{k}_B^4 \Gamma}{\bar{h}^3 v^2} \left(\frac{\pi^4}{15} \right) \tag{12}$$

The most important constant is Γ, a function of the material properties of the two media in contact. Using the figure provided by Little [7], Γ can be obtained if the density ratio and the sound velocity ratio of the two media are known. Chen *et al.* [9] calculated the sound velocity in two ways, from the elastic bulk modulus, and also from the Debye temperature, and suggested that $\Gamma \approx 0.2$ for YBCO/MgO.

Interfacial-layer model

Marshall *et al.* [6] suggested a thermal boundary resistance can be treated as an interfacial layer with low thermal diffusivity. The energy equation, initial, and boundary conditions are as follows [9]:

$$\frac{\partial \theta_l}{\partial \tau} = r_k \left(\frac{\partial^2 \theta_l}{\partial X^2} + \frac{\partial^2 \theta_l}{\partial Y^2} \right) \tag{13}$$

$$\theta_l = 0 \qquad \text{at } \tau = 0 \tag{14}$$

$$\theta_l = \theta_f, \quad -r_k \frac{\partial \theta_l}{\theta X} = -\frac{\partial \theta_f}{\theta X} \qquad \text{at } X = 1 \tag{15a}$$

$$\theta_l = \theta_s, \quad -r_k K_{fs} \frac{\partial \theta_l}{\theta X} = -\frac{\partial \theta_s}{\theta X} \qquad \text{at } X = 1 + r_d \tag{15b}$$

$$\pm \frac{\partial \theta_l}{\partial Y} = \frac{Bi}{r_k \sqrt{K_r}} \theta_l \qquad \text{at } Y = \pm A, \quad 1 < X < 1 + r_d \tag{15c}$$

where r_k is the thermal conductivity ratio of the layer to the film, r_d the thickness ratio of the layer to the film, and subscript l represents the layer.

We used a fully implicit, finite-difference scheme with an under-relaxation technique to solve this conjugate transient heat-conduction problem. Two types of the thermal boundary resistances is also considered. Based on the thin-film temperature solution, the instability parameter can be conveniently calculated for all times after the thermal disturbance is generated. The instability parameter is defined as

$$\Phi = \frac{1}{A} \int_0^1 \int_0^A g(\theta_f) dY dX \tag{16}$$

where

$$g(\theta_f) = \begin{cases} \theta_f, & 0 \le \theta_f \le 1 \\ 1, & \theta_f > 1 \end{cases} \tag{17}$$

The value of φ is directly related to the reduction in current carrying capability. From this parameter we can examine the stability performance of the superconductor. When the relationship between the current density ratio and the instability parameter

$$J_r \le 1 - \Phi(\theta) \tag{18}$$

is satisfied, the superconductor will operate stably at all times during heat diffusion at the dimensionless operating current density ratio J_r determined by the ratio of real current density J_o to critical current density at operating temperature T_o. The critical operating density ratio for intrinsic stability is estimated by

$$(J_r)_{cl} = 1 - \Phi_{max} \tag{19}$$

If the maximum value of instability parameter, φ_{max}, is known, then the critical operating density ratio can be evaluated.

Quench recovery

Analyzing superconductor quench recovery, we can find two important characteristic parameters: the second critical current-density ratio $(J_r)_{c2}$ and the ratio of heat generation rate to the sum of the substrate conductive and convective cooling rates, Q_{rs}. $(J_r)_{c2}$ is a critical value beyond which the stability recovery is impossible after stability fails, and can be determined by considering the temperature distribution within superconductor after the failure of intrinsic stability and the onset of Joule heating. For given operating current density ratio J_r, the intrinsic stability situation is determined by Eq. (18). If $J_r > (J_r)_{c2}$ or $1-\varphi_{max}$, stability will fail when $\varphi = 1-J_r$, and Joule heating is generated. Stability recovery occurs when the heat removed to the substrate and coolant is greater than that generated within superconductor. In other words, when the instability parameter φ is equal to $1-J_r$ again, the Joule heating has disappeared from the superconductor, and intrinsic thermal stability has recovered. The heat conduction equation of thin-film superconductors can be written based on Eq. (4) as

$$\frac{\partial^2 \theta_f}{\partial X^2} + \frac{\partial^2 \theta_f}{\partial Y^2} + \frac{\rho (J_f J_{co} d_f)^2}{k_{fx}(T_c - T_0)} = \frac{\partial \theta}{\partial \tau} \qquad \text{for } \tau_1 \le \tau \le \tau_2 \quad (20)$$

where τ_1, the time when intrinsic stability fails and $\varphi = 1-J_r$ occurs for the first time, and τ_2, the time when the stability recovers and $\varphi = 1-J_r$ occurs for the second time, are dimensionless times. The third term represents the dimensionless Joule heat for the film. σ is normal state electrical resistivity and is assumed to be a constant during the period of operation. We determined $(J_r)_{c2}$ from the steady-state solution of energy Eqs (20) and (5) with boundary condition Eqs (6a–e). This manner for calculating $(J_r)_{c2}$ is the same as that proposed by Unal and Chyu [17]. The numerical method and iterative convergence criterion are similar to those in Eqs (4–15). However, time is disregarded in this case.

In order to study superconductor stability performance, the heat ratio Q_{rs} is defined as

$$Q_{rs} = \frac{q_g}{q_{cv} + q_{cs}} =$$

$$= \frac{\text{heat generation rate per unit–length}}{\text{rates of heat transferred to coolant and substrate per unit–length}} \quad (21)$$

In our analysis, the heat generated in the film includes initial thermal disturbance energy and Joule heat. For $Q_{rs} \cong 1$, the energy is balanced between heat generated in the thin-film superconductor and that conducted to the substrate and coolant.

Results and discussion

For demonstrating the intrinsic thermal stability and quench-recovery behavior of superconducting thin films, we chose a typical system consisting of a $YBa_2Cu_3O_7$ film deposited on a MgO substrate as a base case. Its properties are as follows: $d_f=4$ μm, $a_r=100$, $k_{fx}=0.5$ W mK^{-1}, $K_r=4$, $\sigma=1\times10^{-4}$ Ωm, $J_{co}=1\times10^9$ A m^{-2}, $\rho_f=2720$ kg m^{-3}, $c_f=180.2$ J (kg K)$^{-1}$, and $T_c=95$ K. The system is assumed to be maintained by cooling with liquid nitrogen, to $T_0=77$ K and $h=5\times10^4$ W m^{-2} K^{-1} [2, 19]. The amount of thermal disturbance, $E_d=1$ corresponds to a line source of strength $e_d=2.82\times10^{-8}$ J μm^{-1}. The properties of MgO substrate are listed in Table 1. D is assumed to be 125 for the base case. In this physical model, heat is transferred to both substrate and coolant. Their thermal properties are also important factors that affect the intrinsic thermal stability.

Table 1 Properties of substrates for MgO, $LaAlO_3$ and Sapphire at $T_0=77$ K

Substrate	ρ_s/kg m^3	k_s/W mK	C_s/J kgK
MgO	3580[a]	485.7[a]	88.7[b]
$LaAlO_3$	6520[c]	18.6[c]	14.1[c]
Sapphire	3990[a]	1131[b]	60.7[b]

[a]Slack (1962) [20]
[b]Touloukian and Buyco (1970) [21]
[c]Michael *et al.* (1992) [22]

The influences of thermal boundary resistance on temperature and intrinsic thermal stability are showed in Figs 2 and 3, respectively. Both the ILM and the AMM are employed to calculate the results. $R_{bd}=0$ indicates that no thermal

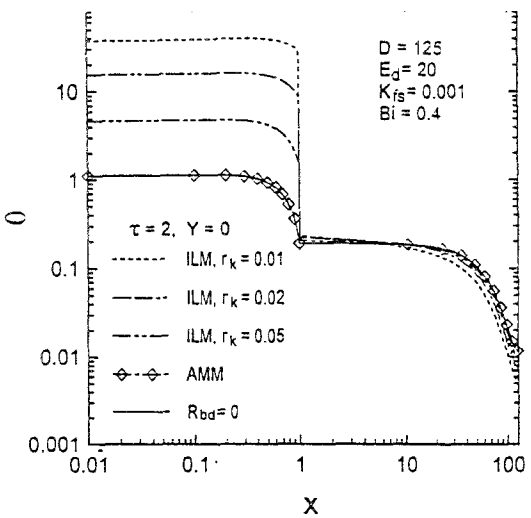

Fig. 2 θ profiles *vs.* X with different thermal boundary resistances at $\tau=2$ and $Y=0$

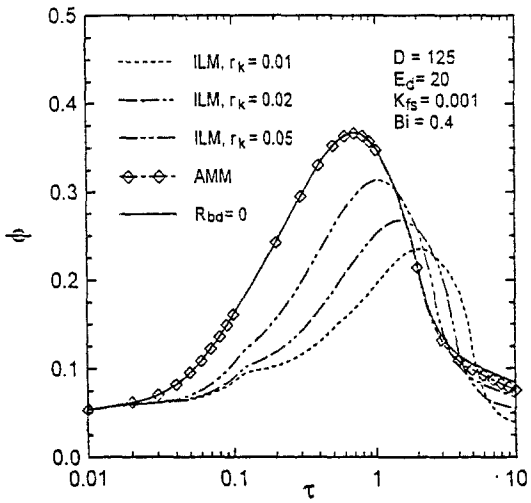

Fig. 3 Effect of different thermal boundary resistances on φ

boundary resistance exists at the interface between film and substrate. Three different cases are discussed for the ILM: r_k=0.01, 0.02 and 0.05 and r_d is set to be 0.01. Marshall *et al.* [6] stated that the rate of flow across the YBCO/MgO interface is ~100 times lower than that across the YBCO film. This corresponds to the case in which r_k=0.01. In Fig. 2, the nondimensional temperature profiles across the film, the interfacial layer, and the substrate at τ=2 and Y=0 are presented. Figure 3 shows the variation of instability parameter φ with the dimensionless time τ.

The difference between the results for using the AMM and those for considering no thermal boundary resistance is trifling in Figs 2 and 3. This means that the AMM exists only a weakly influence on film temperature at 77 K. By contrast, the strong effect of the ILM is depicted in the two figures. Figure 2 displays that the ILM induces an obvious temperature jump at the interface between film and substrate, but the AMM induces only a little of temperature jump so that cannot be observed. The average θ in film for r_k=0.01 is about 30 times larger than that for R_{bd}=0. This implies that ignoring the thermal boundary resistance causes the average film temperature to be greatly underestimated.

The maximum instability parameter, φ_{max}, is the highest for R_{bd}=0 exhibited in Fig. 3. The φ_{max} increases as r_k increase for the ILM. The φ_{max} calculated using the ILM is larger than that obtained using the AMM, indicating that the effects of thermal boundary resistance on stability are more evident when using ILM than when using AMM. A higher thermal boundary resistance gives a lower φ_{max} and increases the time taken to reach the maximum. Besides, this effect make the φ form an abrupt turn point in the neighborhood of τ=0.1. A lower φ_{max} means larger intrinsic critical current density and higher intrinsic thermal stability. Therefore, the stability will increase due to the effects of thermal boundary resistance, because the boundary resistance prevents a large amount of heat from flowing back to the film from the substrate. If the thermal conductivity of substrates is higher than that of

superconducting films, such as in the YBCO/MgO system, heat is conducted in the transverse direction by the substrates more rapidly than by the film. However, this effect will induce a significant feedback of heat from the substrate, especially since the resistance is ignored. From this phenomenon, we know that the growth of normal zone is governed by the feedback heat.

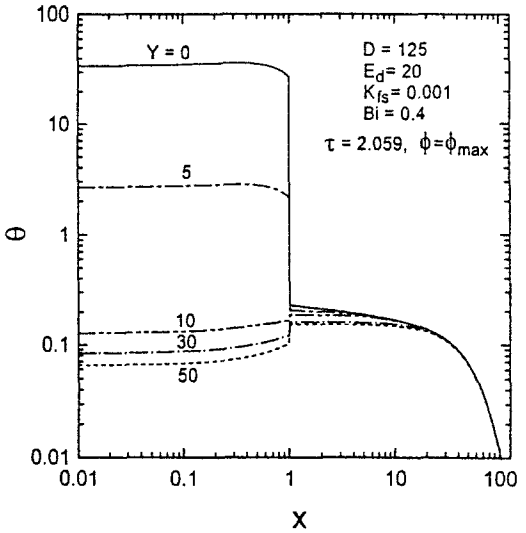

Fig. 4 θ profiles *vs.* *X* with different positions for Y=0, 5, 10, 30 and 50 at τ=2.059 where $\varphi=\varphi_{max}$

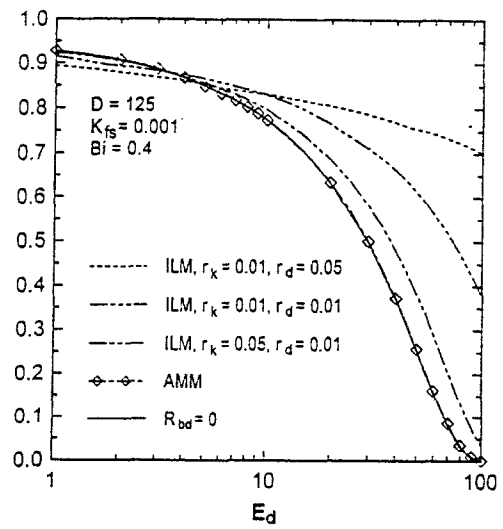

Fig. 5 Influence of different thermal boundary resistances on $(J_r)_{c1}$ dependence of E_d

Figure 4 shows the dimensionless temperature profiles for different positions of Y at $\tau=2.059$, when $\varphi=\varphi_{max}$. The direction of local heat flow can be observed from this figure. As $Y=0$ and 5, the heat transferred from the film to the substrate, and other positions, show contrary heat flow directions. At this time the net heat flux from film to substrate is positive, when $\tau=6.3$, the net heat flux begin to change to a negative value. This means that heat has begun to flow back from the substrate, but this effect does not influence the intrinsic thermal stability. Since the time of the φ_{max} arrived is earlier than that of the negative net heat flux occurred.

The influences of thermal boundary resistances on the relationship between the disturbance energy and the critical current density for intrinsic thermal stability, $(J_r)_{c1}$, are shown in Fig. 5. The $(J_r)_{c1}$ calculated by using the AMM is almost equal to that for $R_{bd}=0$. The results are similar to that presented in Figs 2 and 3. Moreover, it is clear that a large energy release easily induces instability. In other words, higher values of thermal disturbance energy yield higher values of φ_{max} and lower $(J_r)_{c1}$. When considering thermal boundary resistance, the $(J_r)_{c1}$ exerts a higher value for larger E_d. On the contrary, the boundary resistance results in a lower value of $(J_r)_{c1}$ for lower E_d. The main reason is that for a small thermal disturbance, the amount of heat flowing back to the film is slight. This means that the most diffusive region of normal zone or heat is induced by film itself, and at this time the existence of thermal boundary resistance will obstruct the heat from being transferred to the coolant by the substrate. Thus, the stability and $(J_r)_{c1}$ will also decrease due to considering thermal boundary resistance. The different in $(J_r)_{c1}$, between that determined by ignoring thermal boundary resistance and by considering the thermal boundary resistance, decreases with decreasing E_d. Using the ILM, as the r_k decreases or r_d increases, $(J_r)_{c1}$ will rise in proportion for higher E_d and fall for smaller E_d.

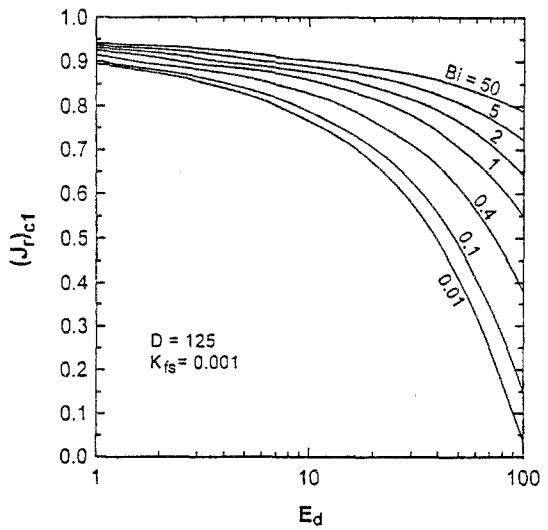

Fig. 6 Influence of Bi on $(J_r)_{c1}$ dependence of E_d

Since the AMM underestimates significantly the thermal boundary resistance at temperatures above ~50 K, we suggest using the ILM. Figure 6 shows the influence of the heat transfer coefficient on $(J_r)_{c1}$ for different disturbance energies according to the ILM. $(J_r)_{c1}$ increases as *Bi* increases, indicating that a higher current density is possible without quenching for larger *Bi*. These results are similar to those for bare film cooled only by coolant [17]. The value of *Bi* represents the capacity to transfer heat to the surrounding coolant. When the rate of heat removed from the superconductor is higher than that of the accumulated energy, which causes the formation of normal zones, the superconductor will remain stable. A larger value of *Bi* obviously promotes $(J_r)_{c1}$ to 0.8~0.9 times the average value for $1 \leq E_d \leq 100$. In this situation thermal disturbance energy affects stability slightly, and the current density carried in the superconductor approaches J_{co}.

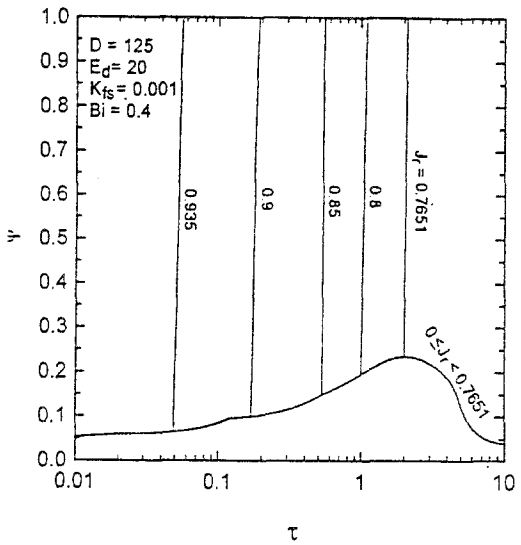

Fig. 7 φ *vs.* τ with different J_r

Figures 7–8 show the performance results of the superconductor subjected to a hypothetical instantaneous disturbance of $E_d=20$. Two important parameters, φ and Q_{rs}, are discussed. Both the conditions of intrinsic thermal stability and quench recovery are considered. These figures show that a superconductor is more likely to be quenched and can not recover when Joule heating occurs. The values of the intrinsic instability parameter φ calculated from Eqs (4), (5) and (20) are presented in Fig. 7. The maximum value of J_r is 0.765094 at $\tau=2.059$, below this the superconductor will operate stably without Joule heating, and intrinsic stability as defined by Eq. (18) is always satisfied, as indicated by $Q_{rs}=0$ in Fig. 8. If the operating current density is higher than 0.765094, the superconductor will be quenched immediately as $J_r=0.7651$, 0.8, 0.85, 0.9 and 0.935. This phenomenon is similar to the results for bare film or tape presented by Unal and Chyu [17]. We also dem-

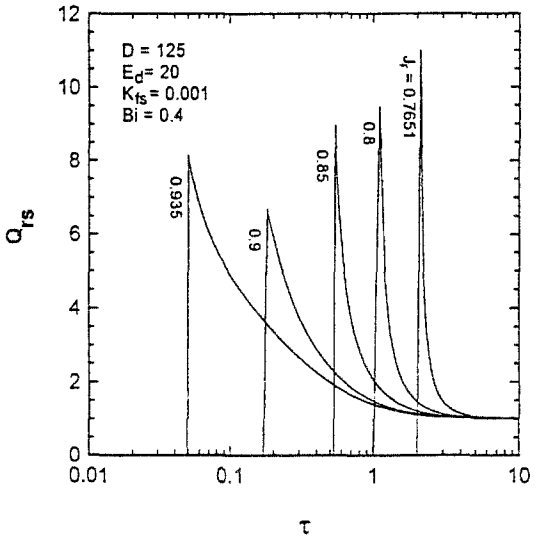

Fig. 8 Q_{rs} *vs.* τ with different J_r

onstrate that isotropic thin-film high-T_c superconductor deposited on a substrate also is either intrinsically stable or irrecoverably unstable under the conditions we assume. In other words, if Joule heat cannot be transferred quickly enough to the substrate and coolant, it will induce irreversible quenching. We also found that higher J_r results in quenching and resistance onset earlier, and that this critical point occurs at $\varphi=1-J_r$.

Variation in the ratio of heat generated in film to heat transferred to substrate and coolant, Q_{rs}, with τ is displayed in Fig. 8. $Q_{rs}\geq 1$ for all $J_r\geq(J_r)_{c1}$ represents the amount of Joule heating is larger than that of heat transferred from film all the times after quenching. The value of Q_{rs} increases sharply because of Joule heat generated abruptly as $\varphi=1-J_r$ is satisfied for a given J_r in film, and arrives simultaneously at the maximum value. Then Q_{rs} decreases as time increases until $Q_{rs}=1$, which represents the energy balance between heat generated in film and that removed from it. This occurs because little heat is conducted to the boundaries at the onset of electric resistance, but increases over time. When $J_r=0.7651$, Q_{rs} exist the maximum value, meaning that the minimum percentage of the heat is being transferred from the film. Joule heating occurs at $\tau=2.1$, 1.1, 0.54, 0.18 and 0.05, respectively, when $J_r=0.7651$, 0.8, 0.85, 0.9 and 0.935. $q_{cv}+q_{cs}$ reaches a maximum value for intrinsic thermal stability at $\tau=0.097$. As J_r increase from 0.7651 to 0.9, both q_g and $q_{cv}+q_{cs}$ increase. But the increase amount of $q_{cv}+q_{cs}$ is higher than that of q_g, so that Q_{rs} is higher for $J_r=0.7651$.

The maximum current density that allows recovery is $(J_r)_{c2}$, which increases with increasing *Bi*, and decreasing K_{fs}, as shown in Figs 9 and 10. The behavior of $(J_r)_{c1}$ is the same as shown in Figs 5 and 6. Unal and Chyu [17] developed the sta-

bility behavior criterion from $(J_r)_{c1}$ and $(J_r)_{c2}$. If $(J_r)_{c1}<(J_r)_{c2}$, three characteristic regions in terms of superconductor stability and recovery have been identified: when $0\leq J_r\leq(J_r)_{c2}$, the superconductor is always stable despite thermal disturbances; when $(J_r)_{c1}<J_r\leq(J_r)_{c2}$, the superconductor can recover stability after quenching; when $J_r>(J_r)_{c2}$, superconductivity fails. If $(J_r)_{c1}\geq(J_r)_{c2}$, two characteristic regions can be identified: when $0\leq J_r\leq(J_r)_{c1}$, the superconductor is stable in spite of the heat disturbance; when $J_r>(J_r)_{c1}$, superconductivity can never be recovered after quenching. According to the definition as stated above, a plot including both $(J_r)_{c1}$ and $(J_r)_{c2}$, such as Figs 9 and 10, is helpful. On these figures, only $(J_r)_{cl}>0$ region is meaningful (when $(J_r)_{c1}=0$, intrinsic thermal stability is impossible for any trifling current). Both figures show that $(J_r)_{c1}$ is greater than $(J_r)_{c2}$ for most K_{fs} and Bi. On the contrary, it is very unlikely that $(J_r)_{c1}\leq(J_r)_{c2}$ and $(J_r)_{c1}\neq 0$. These results demonstrate that the operation of such a superconductor/substrate system under the assumed conditions is either intrinsically stable or irrecoverably unstable.

Figure 9 shows a comparison between $(J_r)_{c1}$ and $(J_r)_{c2}$ for different K_{fs} using the ILM and $R_{bd}=0$. As K_{fs} decreases or k_s increases, not only does the amount of heat feedback increase but the amount of heat transferred to the substrate also increases in a transient process. When $K_{fs}>4\times10^{-4}$, and since the heat diffusive region in films is governed by the heat flowing back into the film, the thermal boundary resistance reduces this effect and increases both $(J_r)_{c1}$ and stability. On the contrary, for smaller K_{fs}, the speed of heat transferred to the coolant by the substrate is much higher than that of heat fed back to the film. This means that an increase in the normal zone, which relies on heat propagated by the film overcomes that caused by heat feedback from the substrate. Therefore, the thermal boundary resistance diminishes the amount of heat directly conducted from the film to the substrate, and increases the diffusive region of the normal zone and decreases $(J_r)_{c1}$. $(J_r)_{c2}$ shows

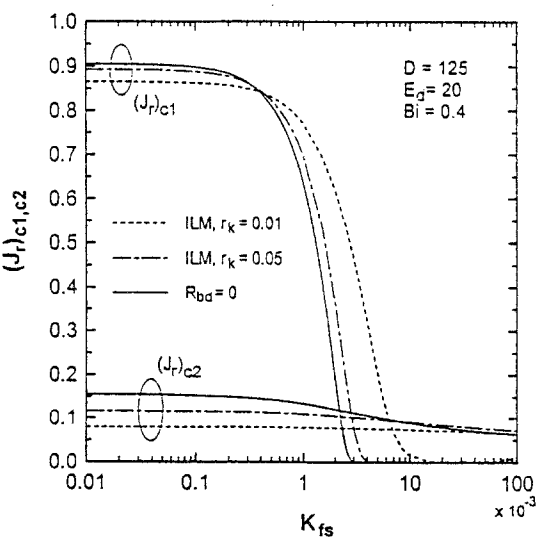

Fig. 9 $(J_r)_{c1}$ and $(J_r)_{c2}$ with various K_{fs} for different thermal boundary resistance

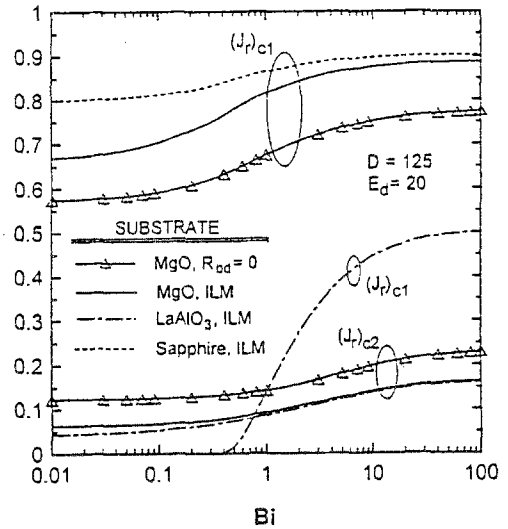

Fig. 10 $(J_r)_{c1}$ and $(J_r)_{c2}$ with different *Bi* for YBCO deposited on three substrates

a slight decrease as K_{fs} increases, because the smaller k_s induces a decrease in heat transferred to the coolant by the substrate. For larger K_{fs} the average temperature of films is higher in the steady state when Joule heating occurs, and thus $(J_r)_{c2}$ is smaller. The effects of the substrate are significantly reduced by thermal boundary resistance. When r_k=0.01 and r_d=0.01, $(J_r)_{c2}$ is almost independent of K_{fs} and it approaches a constant value of about 0.07 when $10^{-5} \leq K_{fs} \leq 0.1$.

The influences of different substrates on the thermal stability, for considering thermal boundary resistance with the ILM where r_k=0.01 and r_d=0.01, is shown in Fig. 10. In this figure, the results of no boundary resistance for MgO is also plotted for comparison. The most common substrates used to deposit high-T_c superconducting film are MgO, $LaAlO_3$ and sapphire. The properties of the substrates are listed in Table 1. The differences between the results for considering finite thermal boundary resistance and those for no boundary resistance are almost independent of *Bi*, and approximately equal to 0.1 and 0.05 for $(J_r)_{c1}$ and $(J_r)_{c2}$, respectively. When the boundary resistance is neglected, $(J_r)_{c1}$ are underestimated, whereas $(J_r)_{c2}$ are overestimated. The reasons are the same as those discussed in Fig. 9.

The critical current density, $(J_r)_{c1}$, for sapphire is the highest, followed by that for MgO, and that for $LaAlO_3$ is the lowest. The main factor leading to different values of $(J_r)_{c1}$ for different substrates is that a high thermal conductivity conducts heat more rapidly to the coolant, and thus decreases the film temperature and the growth of normal zones. The variation in *Bi* from 0.01 to 100 for MgO and sapphire, which have high k_s, only slightly affect $(J_r)_{c1}$. However, the variation in *Bi* has greater influence on $(J_r)_{c1}$ for $LaAlO_3$ which has small thermal conductivity. In other words, the heat transfer capability of coolant produces a significant influence on intrinsic thermal stability only while the thermal conductivity of the substrate is

small. Moreover, this effect also causes that the superconducting film cannot carry any current at $Bi \leq 0.4$ when $(J_r)_{c1}=0$ for $LaAlO_3$ substrate. But for other two substrates, the $(J_r)_{c1}$ decreases asymptotically toward a constant with Bi. The asymptotical values are minimum for a particular substrate, but not equal to zero. Those values are equal to 0.67 and 0.8 for sapphire and MgO substrate, respectively. It means that a large thermal conductivity of substrate can carry a large amount of J_r under a particular thermal disturbance even in the coolant cannot transfer any heat by convection.

The properties of substrates and coolant have only a weak effect on $(J_r)_{c2}$ as shown in Figs 9 and 10. Because $(J_r)_{c2}$ represents the maximum ability of bearing Joule heat for a superconducting film, it has more attractive relationship to the properties of the superconductor's itself than to the environment. $(J_r)_{c2}$ or the three substrates are very close each other for different Bi, indicating that $(J_r)_{c2}$ are almost independent of the properties of the substrate. This result agrees with Fig. 9 which shows that the same boundary resistance model the $(J_r)_{c2}$ almost maintains a constant with different K_{fs}.

Conclusions

The intrinsic thermal stability and quench-recovery of thin-film superconductors deposited on substrates with thermal boundary resistance have been investigated numerically. The thermal boundary resistance models ILM and AMM were used to analyze influences on $(J_r)_{c1}$, the critical current density for quench, and $(J_r)_{c2}$, the critical current density for recovery. The results show that the $(J_r)_{c1}$ is strongly influenced by substrate effects and thermal boundary resistance. The values of $(J_r)_{c1}$ obtained when ignoring the effects of thermal boundary resistance are significantly substrate to film and conducted through the substrate to the coolant are overestimated. By contrast, the variation in $(J_r)_{c2}$ is not significant for different Bi and K_{fs}. From the viewpoint of heat transfer, sapphire was shown to be a better substrate for stably operating superconducting thin films

Nomenclature

a	Half superconductor width (m)
A	Non-dimensional width
A_r	Aspect ratio, a/d_f (dimensionless)
Bi	Biot number (dimensionless)
c	Specific heat (J (kg K)$^{-1}$)
d	Thickness (m)
D	Non-dimensional substrate thickness
e_d	Thermal energy released per unit length (J m^{-1})
E_d	Non-dimensional thermal energy released, $e_d/[2\rho_f c_f(T_c-T_o)ad_f]$
h	Convective heat transfer coefficient (W m^{-2} K^{-1})
$\hbar$	Planck's constant$=6.6262\times10^{-34}$ J s
J	Current density (A m^{-2})

J_r Current density ratio, J_o/J_{co} (dimensionless)
$(J_r)_c$ Critical current density ratio at the point where $(J_r)_{c1}=(J_r)_{c2}$
$(J_r)_{c1}$ Critical current density ratio for intrinsic stability (dimensionless)
$(J_r)_{c2}$ Critical current density ratio for recovery (dimensionless)
k Thermal conductivity (W m K^{-1})
k_B Boltzmann constant=1.38062×10^{-23} J K^{-1}
K Non-dimensional thermal conductivity
K_{fs} Ratio of thermal conductivity, k_{fx}/k_s
K_r Ratio of thermal conductivity, k_{fy}/k_{fx}
K Thermal conductivity tensor
q Heat rate per unit length (W m^{-1})
q_b Boundary heat flux
Q_b Non-dimensional boundary heat flux
Q_{rs} Ratio of heat generation rate to heat rate brought out from film, $q_g/(q_{cv}+q_{cs})$
r_d Thickness ratio of interfacial layer to film
r_k Thermal conductivity ratio of interfacial layer to film
R_{bd} Thermal boundary resistance
T Temperature (K)
t Time (s)
v Sound velocity (m s^{-1})
x, y Cartesian coordinate
X, Y Transformed dimensionless coordinate

Greek letters

α Thermal diffusivity (m^2 s^{-1})
Γ Constant; see Eq. (12)
φ Instability parameter (dimensionless)
κ Constant; see Eq. (12)
θ Non-dimensional temperature, $(T-T_o)/(T_c-T_o)$
ρ Density (kg m^{-3})
σ Normal state electrical resistivity (Ω m)
τ Non-dimensional time, $k_{fy}t/(d^2\rho C)_f$

Subscripts

1, 2 Point of intrinsic thermal stability failure and recovery, respectively
c Critical
co Critical operation
cv Convection by coolant
cs Conduction by substrate
f Film
l Interfacial layer
max Maximum
o Operating
r Ratio
s Substrate
x, y In *x, y* direction

The authors wish to express their sincere appreciation to Dr. R. C. Chen for his invaluable advice and suggestions during the course of this paper. This research was supported by the National Science Council of the R. O. C. through grant NSC 83-0401-E-009-006. The computations were performed on the IBM ES/9000 at the National Center For High-Performance Computing.

References

1 M. N. Wilson, Superconducting magnets. Clarendon Press, Oxford, UK 1983.
2 M. I. Flik and C. L. Tien, ASME J. Heat Transfer, 112 (1990) 10.
3 M. Wetzko, M. Zahn and H. Reiss, Cryogenics, 35 (1995) 375.
4 S. K. Streiffer, B. M. Lairson, C. B. Eom, B. M. Clemens, J. C. Bravman and T. H. Geballe, Phys. Rev. B, 43 (1991) 13007.
5 E. T. Swartz and R. O. Pohl, Rev. Mod. Phys., 61 (1989) 605.
6 C. D. Marshall, I. M. Fishman, R. C. Dorfman, C. B. Eom and M. D. Fayer, Phys. Rev. B, 45 (1992) 10009.
7 W. A. Little, Can. J. Phys., 37 (1959) 334.
8 M. Nahum, S. Verghese and P. L. Richards, Appl. Phys. Lett., 59 (1991) 2034.
9 R. C. Chen, J. P. Wu and H. S. Chu, ASME J. Heat Transfer, 117 (1995) 366.
10 Z. J. Stekly and J. L. Zar, IEEE Trans. on Nuclear Science, 12 (1965) 367.
11 L. Dresner, Cryogenics, 16 (1976) 675.
12 B. Turck, Cryogenics, 20 (1980) 146.
13 A. Devred, J. Appl. Phys., 67 (1990) 7467.
14 Z. P. Zhao and Y. Iwasa, Cryogenics, 31 (1991) 817.
15 S. Y. Seol and M. C. Chyu, Cryogenics, 34 (1994) 521.
16 R. C. Chen and H. S. Chu, Cryogenics, 31 (1991) 749.
17 A. Unal and M. C. Chyu, Cryogenics, 34 (1994) 123.
18 S. Y. Seol and M. C. Chyu, Cryogenics, 34 (1994) 513.
19 S. J. Hagen, Z. Z. Wang and N. P. Ong, Phys. Rev. B, 40 (1989) 9389.
20 G. A. Slack, Phys. Rev., 126 (1962) 427.
21 Y. S. Touloukian and E. H. Buyco, Thermal physical properties of matter Vol. 5. IFI/Plenum, New York 1970.
22 P. C. Michael, J. U. Trefny and B. Yarar, J. Appl. Phys., 72 (1992) 107.